EUROPEAN ORGANIZATION FOR NUCLEAR RESEARCH

CERN-PPE/ 97-139
25.9.97

Direct evidence for stability of tetrahedral interstitial Er in Si up to 900°C

U. Wahl[1], J.G. Correia[2], G. Langouche[1], J.G. Marques[3],
A. Vantomme[1], and the ISOLDE collaboration[2]

[1] *Instituut voor Kern- en Stralingsfysica, University of Leuven, Celestijnenlaan 200 D, B-3001 Leuven, Belgium*

[2] *CERN-PPE, CH-1211 Geneva 23, Switzerland*

[3] *CFNUL, Av. Prof. Gama Pinto 2, P-1699 Lisboa Codex, Portugal*

Abstract

Conversion electron emission channeling from the isotope ^{167m}Er (2.28 s), which is the decay product of radioactive ^{167}Tm (9.25 d), offers a means of monitoring the lattice sites of Er in single crystals. We have used this method to determine the lattice location of ^{167m}Er in Si directly following room temperature implantation of ^{167}Tm, after subsequent annealing steps, and also in situ during annealing up to 900°C. Following the recovery of implantation damage around 600°C, about 90% of Er occupies near-tetrahedral interstitial sites in both FZ and CZ Si. While in FZ Si ^{167m}Er was found to be stable on these sites even at 900°C, the tetrahedral Er fraction in CZ Si decreased considerably after annealing for 10 min at 800°C and above.

(IS 342)

(Presented at 19th International Conference on Defects in Semiconductors, Aveiro, Portugal, 21.-25.7.97
in shortened form Phys. Rev. Lett. 79 (1997) 2069.)

DIRECT EVIDENCE FOR STABILITY OF TETRAHEDRAL INTERSTITIAL Er IN Si UP TO 900°C

U. Wahl[1], J.G. Correia[2], G. Langouche[1], J.G. Marques[3], A. Vantomme[1], and the ISOLDE collaboration[2]

[1] Instituut voor Kern- en Stralingsfysica, University of Leuven, Celestijnenlaan 200 D, B-3001 Leuven, Belgium, email: ulrich.wahl@fys.kuleuven.ac.be

[2] CERN-PPE, CH-1211 Genève 23, Switzerland

[3] CFNUL, Av. Prof. Gama Pinto 2, P-1699 Lisboa Codex, Portugal

Abstract

Conversion electron emission channeling from the isotope ^{167m}Er (2.28 s), which is the decay product of radioactive ^{167}Tm (9.25 d), offers a means of monitoring the lattice sites of Er in single crystals. We have used this method to determine the lattice location of ^{167m}Er in Si directly following room temperature implantation of ^{167}Tm, after subsequent annealing steps, and also in situ during annealing up to 900°C. Following the recovery of implantation damage around 600°C, about 90% of Er occupies near-tetrahedral interstitial sites in both FZ and CZ Si. While in FZ Si ^{167m}Er was found to be stable on these sites even at 900°C, the tetrahedral Er fraction in CZ Si decreased considerably after annealing for 10 min at 800°C and above.

Introduction

Despite an impressive success in manufacturing light-emitting diodes from Er-doped Si [1-3], the microscopic structure and detailed luminescence mechanisms of Er in Si are still a matter of debate. This includes in particular the lattice sites of Er and the role of possible light element ligands such as C, N, O or F which were found to intensify the luminescence yield [4]. Theoretical investigations [5] predict that tetrahedral interstitial (T) sites are the most stable sites for all oxidation states of isolated Er atoms in Si, while substitutional (S) and hexagonal interstitial (H) sites should be metastable. Direct lattice location using the Rutherford backscattering (RBS) channeling technique, however, only suggested Er on S [6] or H [7,8] sites. Photoluminescence (PL) spectroscopy studies have identified a number of Er defects with different symmetry properties in Si [9,10]. The most intense PL yield resulted from two centers having cubic and axial symmetry, respectively. The cubic center occurred in both float-zone (FZ) and Czochralski (CZ) Si and was attributed to tetrahedral interstitial Er, while the center with axial symmetry was characteristic to CZ Si and ascribed to Er-O complexes [10]. Possible explanations for several other PL centers of lower symmetry, observed mainly in Si annealed at lower temperatures (600°C), were Er on H sites [9], Er paired with implantation-induced defects [10], and recently also Er on S sites [11]. Different atomic surroundings of Er in FZ Si and CZ Si were clearly revealed by studying its extended X-ray absorption fine structure (EXAFS) [12,13]. In FZ Si and 600°C-annealed CZ Si, EXAFS observed Er surrounded by 6-12 Si atoms at distances around 3.0 Å. This can be explained by the majority of Er in Er_3Si_5 or $ErSi_2$ silicide phases, where 10, respectively 12, nearest neighbour (NN) Si atoms are at 2.99 Å. However, isolated Er on T sites with 4 NN at 2.35 Å and 6 next-nearest neighbours (NNN) at 2.72 Å, or on H sites (6 NN at 2.25 Å, 8 NNN at 3.53 Å) cannot be ruled out taking into account possible relaxations of surrounding Si atoms, while Er on S sites (4 NN at 2.35 Å, 12 NNN at 3.84 Å) seems less probable. In contrast to this, Er in O-implanted or CZ Si annealed to 900°C was characterized by Er_2O_3-like surroundings with 5-6 nearest O neighbours at distances around 1.5-2.5 Å.

We report on direct lattice location of Er in Si using the emission channeling technique [14], which makes use of the fact that charged particles emitted from radioactive isotopes in a single crystal experience channeling or blocking effects along crystallographic axes and planes. This leads to an anisotropic emission yield from the crystal surface, which depends in a characteristic way on the

occupied lattice sites of the probe atoms. Previously [15], we have already applied this method to study Er in CZ Si. In the present contribution we focus on results in FZ Si and compare both types of Si.

Experiment

For lattice location of Er we monitored the angular-dependent emission yield of the combined intensity of 150, 199 and 206 keV conversion electrons emitted from the nucleus ^{167m}Er ($t_{1/2}$=2.28 s). This isomeric state is populated as a result of the decay of radioactive ^{167}Tm ($t_{1/2}$=9.25 d). The isotope ^{167}Tm was produced at the ISOLDE facility [16] at CERN. We investigated four different samples, *p*-Si:B FZ (10 kΩcm, <111> surface orientation, implanted dose 4.8×10^{13} cm^{-2}), *n*-Si:P FZ (>4 kΩcm, <111>, 5.1×10^{13} cm^{-2}), *p*-Si:B CZ (<100>, 5-14 Ωcm, 4.4×10^{13} cm^{-2}) and *n*-Si:P CZ (<100>, 1-10 Ωcm, 3.5×10^{13} cm^{-2}). All samples were initially dipped into HF to remove native oxide layers. Following 60 keV room temperature implantation of ^{167}Tm, the *n*-Si CZ crystal was annealed in an external vacuum furnace at <10^{-5} mbar, while thermal treatment of all other samples took place in the channeling setup at <10^{-6} mbar by means of a W filament for radiative heating up to 900°C. The conversion electron emission yield as a function of the angle from different crystallographic directions was measured using a position-sensitive Si "pad" detector [17], consisting of 22×22 pads (or pixels) of 1.3×1.3 mm^2 size and mounted at a distance of 285 mm from the sample.

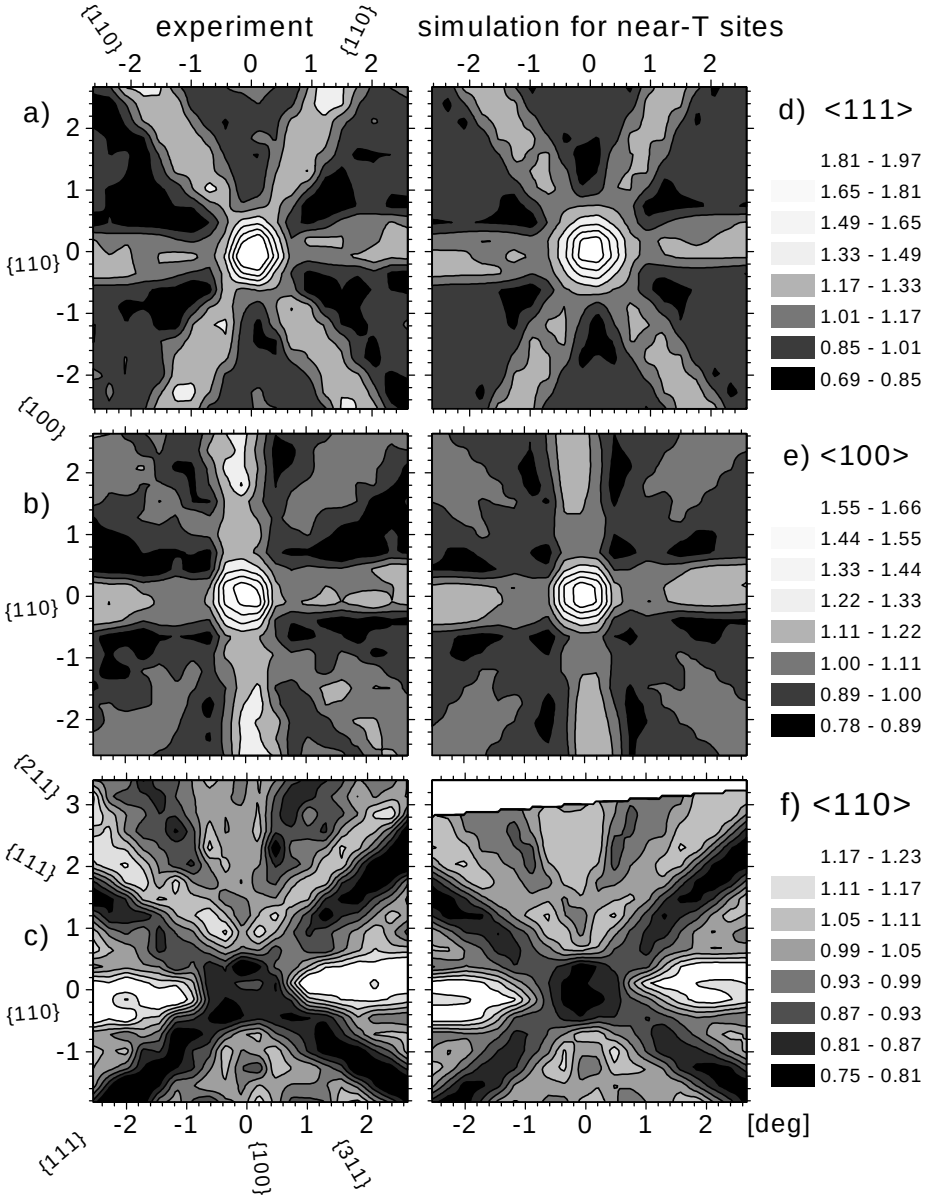

Fig. 1. a), b), c): channeling patterns from ^{167m}Er in *n*-Si FZ annealed at 600°C for 10 min. Normalized electron emission yields in the vicinity of <111>, <100> and <110> directions are shown. **d), e), f):** best fits of simulated patterns to the experimental yields, corresponding to 94%, 99% and 95% of emitter atoms on sites which are displaced by 0.43 Å from the T site.

Results and Discussion

Figures 1a, 1b and 1c show the normalized emission yield of conversion electrons from ^{167m}Er, measured at 20°C after annealing the *n*-Si FZ crystal at 600°C for 10 min. Clearly visible are channeling effects along axial <100> and <111> and planar {110}, {100} and {211}, while axial <110> and planar {111} and {311} directions all show yields close to or below unity. The combination of these patterns provides direct evidence that the majority of ^{167m}Er occupies sites close to the tetrahedral interstitial position. The T sites are perfectly aligned with <100>, <111>, {110}, {100} and {211} lattice directions, leading to channeling of electrons emitted from these sites, but they are off the <110> atomic axes and {111} and {311} atomic planes, causing yield minima along these directions. In order to extract more specific information, the experimental patterns are compared to theoretical emission yields for a variety of different lattice sites. The basic principles of computer simulations of electron emission channeling are discussed in Ref. [14]. More detailed information on calculations for ^{167m}Er in Si and on the fitting procedures for comparison of theoretical and experimental patterns were given in Ref. [15]. Note that the fitting procedures are only slightly modified versions of those used already for alpha emission channeling [18].

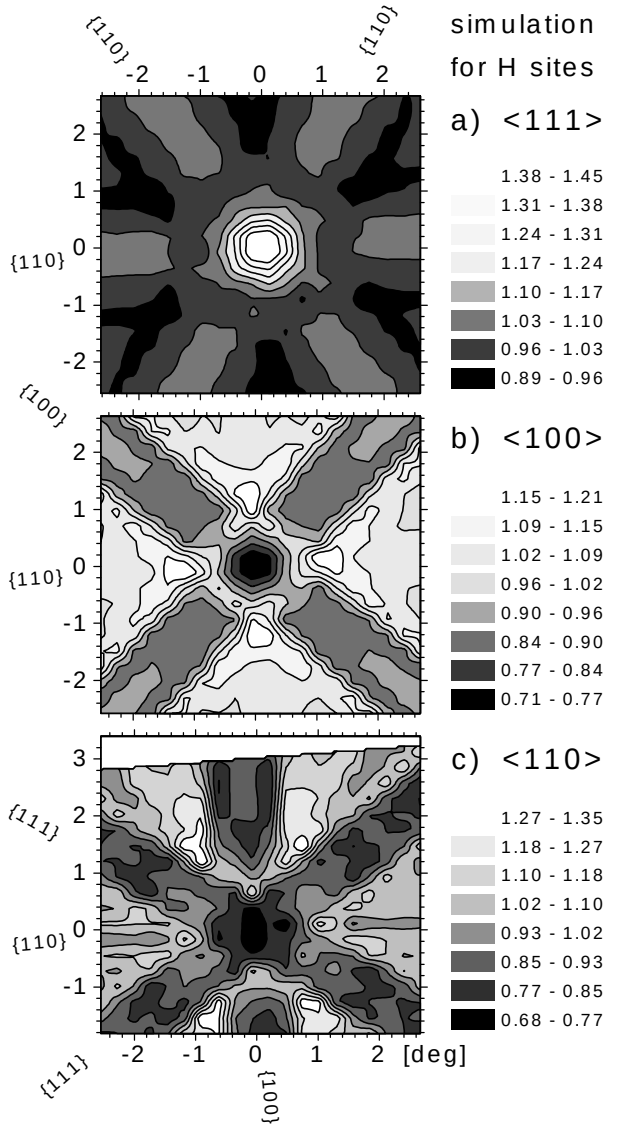

Fig. 2. Calculated patterns for 100% of ^{167m}Er on H sites, choosing the same orientation and angular resolution as used in the fits in Fig. 1.

The experimental data shown in Fig. 1 can be well described by assuming only one type of Er lattice site and a small so-called "random" fraction, the latter responsible for an isotropic electron emission yield. Under these assumptions, best fit results are obtained for nearly 100% of emitter atoms on sites which are 0.43(8) Å displaced from the tetrahedral interstitial T site. Note that ideal T sites would yield much more pronounced <111> and <100> channeling effects. Therefore ideal T sites cannot satisfactorily fit the experimental patterns, leading to a >30% increase in the chi square value. However, the fit quality is not particularly sensitive to the direction of the displacement, and displacements along <111> and <100> give similar results. Allowing for contributions from more than one site does not significantly improve fit quality, while comparable chi square values can usually be obtained for several combinations of lattice sites in the range d≈0-0.6 Å from the T sites. This behaviour is not astonishing since in case of small displacements the channeling effect mainly senses the projected mean displacement of the emitter atoms. On the other hand, significant Er fractions on sites further away from T sites can

be ruled out, since these exhibit entirely different emission patterns. This is illustrated for the case of H sites in Fig. 2, where characteristic changes compared to T sites are the emission minima along <100> and {100} directions. This is due to the fact that H sites are located off all atomic <100> axes and {100} planes. Note that the <111> and <100> patterns of bond center (BC) and anti-bonding (AB) sites are completely identical to H sites. If existing at all, the Er fraction on substitutional sites must also be small. Only the <110> pattern (Fig. 1c) allows to discriminate between S and T sites. Slight improvements in <110> fit quality indicated possible fractions of up to 5% on S sites, however, this value is close to the statistical limit of the data.

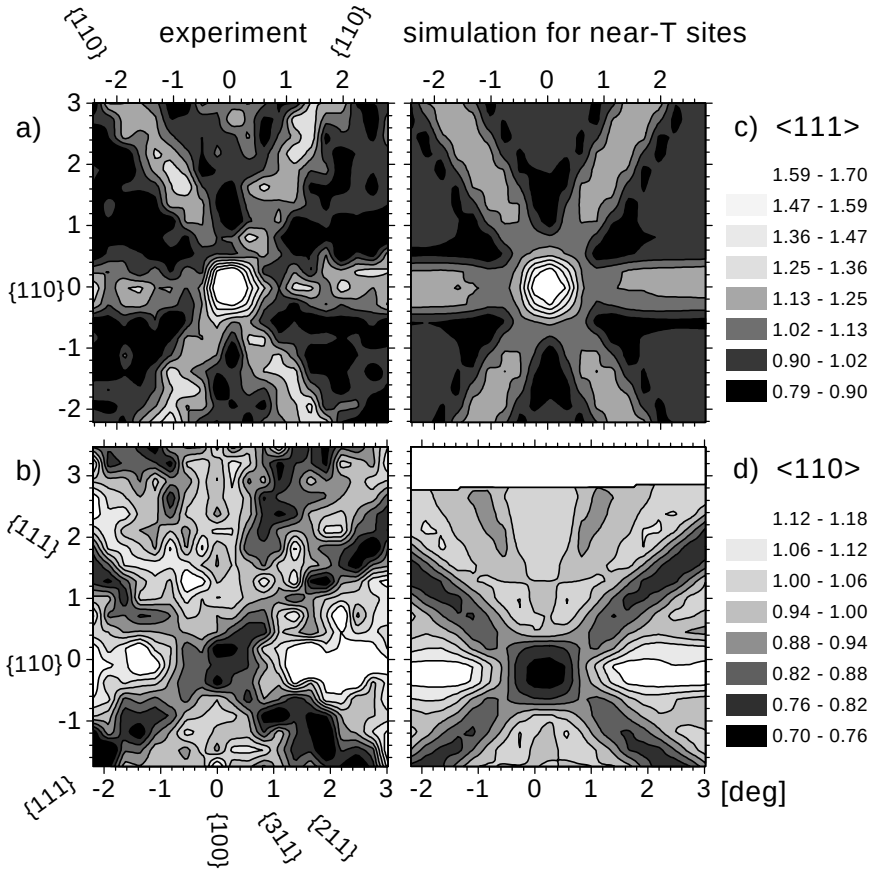

Fig. 3. a), b): <111> and <110> channeling patterns from ^{167m}Er in *n*-Si FZ measured at 900°C. **c), d):** best fits of simulated patterns to the experimental yields, corresponding to 95% and 87% of emitter atoms on near-T sites.

We can not a priori exclude that the observed ^{167m}Er lattice sites are already completely determined by the chemical nature of the parent Tm. The influence of the electron capture decay of ^{167}Tm is hard to predict. The ^{167}Er nucleus receives a recoil energy of 0.7 to 0.9 eV due to neutrino emission, and the initial electronic configuration of Er contains a hole in the K shell. Both thermalization of nuclear recoil and electronic deexcitation via X-ray emission are finished when the conversion electrons are emitted, but could have produced metastable configurations. We have therefore chosen to directly monitor the thermal stability of near-tetrahedral ^{167m}Er by increasing the measuring temperature. Recording emission channeling patterns while keeping the *n*-Si FZ sample at 600°C and 900°C, we obtained essentially the same results as at room temperature (Figs. 3 and 4). This gives direct evidence that Er is stable on the near-T sites up to 900°C, at least during the 2.28 s time window of the half life of the isomeric state.

Figure 4 displays the Er fractions on near-T sites following isochronal annealing steps of both FZ and CZ Si. Electron emission channeling effects were already clearly visible directly after room temperature implantation. The channeling patterns could be well fitted by assuming 20-25% of Er on near-T sites and the others contributing with an isotropic emission yield. Isotropic emission yields are characteristic for probe atoms on sites of very low crystal symmetry or in amorphous surroundings. Since the ^{167}Tm/^{167}Er probes end up in highly defective crystalline surroundings, we believe that in the as-implanted state the fraction of probe atoms which are located near tetrahedral interstitial positions with only short-range order preserved, is much higher than 20-25%. Upon

annealing to 600°C, electron emission channeling effects increased markedly. We attribute this to the well-known solid phase epitaxial regrowth of implanted Si in the temperature range 550-600°C (see, e.g., Ref. [19]). As a result, the quality of the crystal lattice is restored to a large extent, and our measurements show that subsequently more than 90% of ^{167}Er emitter atoms are located on near-T sites. For annealing above 800°C, the fraction on near-T sites dropped markedly in CZ Si. However, this decrease was not compensated by an increase of other specific lattice sites but was rather due to the occupancy of random sites. In contrast, even prolonged annealing at 900°C for 2h could not reduce the near-T fraction in FZ Si by more than 10%.

Comparing with RBS studies reported in the literature, our results correspond with the near-T sites assigned to Yb in Si [20,21], Er in GaAs [22,23] and Er in highly doped AlGaAs [23], but differ from the H sites reported for Er in 600°C-annealed CZ Si [8,9], S sites for Er in unspecified Si [7], and S sites for Er in low-doped AlGaAs [23]. Possible reasons for the discrepancy in the case of CZ Si could be the higher Er doses applied in the RBS experiments combined with hot implantation at 350°C, or the influence of nuclear decay in our experiments. However, since the RBS data shown in Refs. [8,9] closely resemble those in Refs. [22,23], we suggest that the interpretation as H sites is questionable and the authors of [8,9] also observed near-T sites.

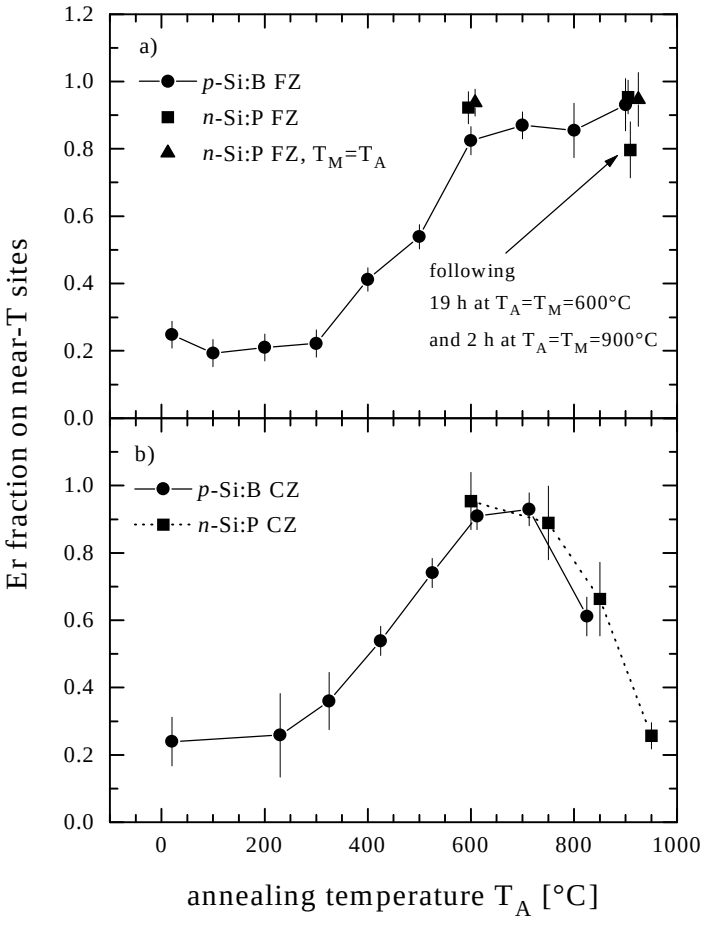

Fig. 4. Isochronal annealing sequences (10 min) for the fraction of ^{167m}Er on near-T sites in FZ and CZ Si. All measurements were done at room temperature, except for those marked $T_M=T_A$, where measuring and annealing temperature were identical.

What could be the reasons for the decrease in the near-T Er fraction in CZ Si? The Tm/Er concentration reaches a maximum of 2×10^{19} cm^3 in the peak of the implantation cascade, which is about a factor of 20 or more higher than the usual O concentrations in CZ Si. From the diffusivity of O ($D=0.13$ cm^2 s^{-1} exp[-2.53 eV/kT] [24]) one estimates migration lengths of 110 Å within 10 min at 600°C and 8100 Å at 900°C. Therefore, a few simple O-Tm and O-Er pairs might already form at moderate annealing temperatures. Complexes where all Tm/Er atoms are saturated with multiple oxygen atoms, however, would require prolonged annealing since the additional oxygen has to be supplied by the bulk of the sample. At 900°C the diffusivity of Er ($D\approx10^{-15}$ cm^2 s^{-1} [1]) also plays a role, giving mean diffusion lengths of 190 Å within 10 min. The parent Tm probably acts similar to Er. The following scenario is compatible with both our observations in CZ Si and the EXAFS results of Refs. [12,13]. Some Er atoms capture oxygen already around 600°C, probably still residing on near-T sites. Upon further annealing to 900°C these centers act as precipitation nuclei for additional oxygen supplied by the bulk and the remaining rare earths, forming disordered Er_2O_3-like precipitates.

Conclusions

Our experiments give direct evidence that Er can be incorporated close to tetrahedral interstitial sites in Si, as was already suggested by the existence of a cubic PL center [9,10] and is in accordance with theoretical predictions [5]. However, we observed either static displacements of 0.43(8) Å from ideal T sites for all Er atoms, or, equally possible, the existence of several different Er lattice sites in the range 0-0.6 Å from the T sites. Our interpretation is that there exists a mixture of Er on ideal T sites and some displaced Er paired with nearby vacancies or other defects. In contrast to FZ Si, where near-T Er shows a remarkable thermal stability even at 900°C, the near-T fraction of ^{167m}Er in CZ Si decreases considerably for 10 min annealing at 800°C and above. We therefore suggest that segregation of Er and O into small disordered rare earth oxide precipitates accompanies the increase in luminescence yield which is usually observed for Er-doped CZ Si annealed at 900°C.

Acknowledgments

We thank the ISOLDE collaboration for providing the radioactive isotopes used in this study, and H. Hofsäss for the permission to use his electron channeling simulation code "Manybeam". J.G.M. and J.G.C. acknowledge JNICT (Portugal) for grants under the Praxis XXI program, A.V. the post-doctoral research program of the Fund for Scientific Research, Flanders (FWO).

References

[1] F.Y.G. Ren, J. Michel, Q. Sun-Paduano, B. Zheng, H. Kitagawa, D. C. Jacobson, J. M. Poate and L. C. Kimerling, Mat. Res. Soc. Symp. Proc. **301**, 87 (1993).
[2] G. Franzo, F. Priolo, S. Coffa, A. Polman and A. Carnera, Appl. Phys. Lett. **64**, 2235 (1994).
[3] B. Zheng, J. Michel, F.Y.G. Ren, L.C. Kimerling, D. C. Jacobson and J. M. Poate, Appl. Phys. Lett. **64**, 2842 (1994).
[4] J. Michel, J.L. Benton, R.F. Ferrante, D.C. Jacobson, D.J. Eaglesham, E.A. Fitzgerald, Y.H. Xie, J.M. Poate and L.C. Kimerling, J. Appl. Phys. **70**, 2672 (1991).
[5] M. Needels, M. Schlüter and M. Lannoo, Phys. Rev. B **47**, 15533 (1993).
[6] Y. S. Tang, Z. Jingping, K. C. Heasman and B. J. Sealy, Sol. State Comm. **72**, 991 (1989).
[7] A. Kozanecki, R. Wilson, B. J. Sealy, J. Kaczanowski, and L. Nowicki, Appl. Phys. Lett. **67**, 1847 (1995).
[8] A. Kozanecki, J. Kaczanowski, R. Wilson and B. J. Sealy, Nucl. Instr. Meth. B **118**, 709 (1996).
[9] Y.S. Tang, K.C. Heasman, W.P. Gillin, and B.J. Sealy, Appl. Phys. Lett. **55**, 432 (1989).
[10] H. Przybylinska, W. Jantsch, Y. Suprun-Belevitch, M. Stephikhova, L. Palmetshofer, G. Hendorfer, A. Kozanecki, R. J. Wilson and B. J. Sealy, Phys. Rev. B **54**, 2532 (1996).
[11] S.Y. Ren and J.D. Dow, J. Appl. Phys. **81**, 1877 (1997).
[12] D.L. Adler, D.C. Jacobson, D.J. Eaglesham, M.A. Marcus, J.L. Benton, J.M. Poate and P.H. Citrin, Appl. Phys. Lett. **61**, 2181 (1993).
[13] A. Terrasi, G. Franzo, S. Coffa, F. Priolo, F. D'Acapito and S. Mobilio, Appl. Phys. Lett. **70**, 1712 (1997).
[14] H. Hofsäss and G. Lindner, Phys. Rep. **201**, 123 (1991).
[15] U. Wahl, J.G. Correia, J. De Wachter, G. Langouche, J.G. Marques, R. Moons, A. Vantomme, and the ISOLDE collaboration, Mat. Res. Soc. Symp. Proc. **469** (1997), in press.
[16] E. Kugler, D. Fiander, B. Jonson, H. Haas, A. Przewloka, H.L. Ravn, D.J. Simon, K. Zimmer and the ISOLDE collaboration, Nucl. Instr. Meth. B **70**, 41 (1992).
[17] P. Weilhammer, E. Nygård, W. Dulinski, A. Czermak, F. Djama, S. Gadomski, S. Roe, A. Rudge, F. Schopper and J. Strobel, Nucl. Instr. Meth. A 383, **89** (1996).
[18] U. Wahl, S.G. Jahn, M. Restle, C. Ronning, H. Quintel, K. Bharuth-Ram, H. Hofsäss, and the ISOLDE collaboration, Nucl. Instr. Meth. B **118**, 76 (1996).
[19] E. Rimini, *Ion Implantation: Basics to Device Fabrication*, Kluwer, Boston, 1995, p 173 ff.
[20] J.U. Andersen, O. Andreasen, J.A. Davies and E. Uggerhøj, Radiat. Effects **7**, 25 (1971).
[21] F. H. Eisen and E. Uggerhøj, Radiat. Effects **12**, 233 (1972).

[22] J. Nakata, M. Taniguchi and K. Takahei, Appl. Phys. Lett. **61**, 2665 (1992).
[23] E. Alves, M.F. da Silva, A.A. Melo, J.C. Soares, G.N. van den Hoven, A.Polman, K.R. Evans and C.R. Jones, Mat. Res. Soc. Symp. Proc. **301**, 175 (1993).
[24] Landolt-Börnstein, Numerical Data and Functional Relationships in Science and Technology, Vol. 22b, edited by M. Schulz (Springer, Berlin, 1989).